



Synthesis and Characterization of Thallium Containing Bismuth Based Superconducting Materials

RASHID MAHMOOD^{1,*} and MUHAMMAD JAVED IQBAL²

¹Department of Chemistry, University of Azad Jammu and Kashmir, Chela Campus, Muzaffarabad-13100, Pakistan

²Preston Institute of Nanoscience and Technology, Preston University, H-8, Islamabad, Pakistan

*Corresponding author: E-mail: rashid_meh786@yahoo.com

Received: 9 January 2015;

Accepted: 19 February 2015;

Published online: 22 June 2015;

AJC-17356

Bismuth based superconducting materials doped with thallium having a general formula $\text{Bi}_{2-x}\text{Tl}_x\text{Pb}_{0.4}\text{Sr}_2\text{Ca}_2\text{Cu}_3\text{O}_y$ ($x = 0.00, 0.05, 0.15, 0.25$ and 0.35) were synthesized by the simple solid state reaction method. The effect of doping of thallium at the Bi-site, on the microstructure, electric and magnetic properties has been investigated through resistivity-temperature data, ac magnetic susceptibility and X-ray diffraction (XRD) analysis. It has been observed that the sample with thallium content, $x = 0.25$ has minimum room temperature resistivity value of 0.012 (ohm-cm) amongst all the samples studied here. The samples with $x = 0.25$ and 0.35 both have shown the highest $T_{c(0)} \sim 109$ K which is 4 K higher than that of the undoped sample. All of the samples were found to consist of both high-Tc (2223) and low-Tc (2212) phases in different proportions.

Keywords: Superconductivity, Bi (2223) materials, Thallium, Electrical resistivity.

INTRODUCTION

The Bi-Sr-Ca-Cu-O system does not contain any rare earth element and is environmentally more stable than its predecessor, the Y-Ba-Cu-O system¹. Three superconducting phases exist in the Bi-based superconducting oxide family. A lot of interest has been focused on the phase with the highest T_c (110K) in the system, namely Bi (2223) phase². Doping of the HTS materials can play an important role in understanding the complex properties of the superconducting materials³. It has been reported that the addition of Pb greatly facilitates Bi (2223) phase formation by conventional route starting from oxides and carbonates⁴. For system $\text{Bi}_{2-x}\text{V}_x\text{Sr}_2\text{Ca}_2\text{Cu}_3\text{O}_y$ ($x = 0-1$), the high- T_c (2223) phase is reported to increase with an increase in concentration of vanadium at the expense of the low- T_c phase (2212)⁵. For $\text{Bi}_2\text{Pb}_{1-x}\text{Sn}_x\text{Sr}_2\text{Ca}_2\text{Cu}_3\text{O}_y$ ($x = 0.0-0.3$), Sn helps the formation of high- T_c phase and a minor elevation in T_c , at lower concentration range $x < 0.1$. However at higher Sn contents ($0.1 \leq x \leq 1$), Sn does not significantly affect the formation of 2223 phase⁶. It has been suggested that the replacement of Bi^{3+} by Pb^{2+} draws electronic charges out of the CuO_2 layers and increases the oxygen hole (charge carrier) in these layers⁷. A lead-tin combination is reported to be effective in promoting the 110 K phase as compared to the Pb or Sn doped Bi (2223) systems⁸. The position of the diffraction peaks in the high- T_c phase is reported to shift to lower diffraction angles with an increase of V_2O_5 contents. This observation

suggests that by increasing V_2O_5 content the lattice parameters are increased owing to incorporation of V ions at the interstitial site in the unit lattice rather than their substitution for copper, Bi^{3+} or Pb^{2+} ions⁹. Addition of TiO_2 in $(\text{BiPb})_2\text{Sr}_2\text{Ca}_2\text{Cu}_3\text{O}_{10-6}$ results in the formation of SrTiO_3 and a decrease of the amount of the Bi (2223) phase¹⁰. Increase in Nb concentration at Bi and Cu-sites in $(\text{BiPb})_2\text{Sr}_2\text{Ca}_2\text{Cu}_3\text{O}_y$ system results into a decrease in $T_{c(0)}$ ¹¹.

In the present study, a series of $\text{Bi}_{2-x}\text{Tl}_x\text{Pb}_{0.4}\text{Sr}_2\text{Ca}_2\text{Cu}_3\text{O}_y$ samples having different thallium content ($x = 0.0-0.35$) were prepared by the simple solid state technique¹². The values of $T_{c(0)}$, $T_c^{(\text{onset})}$ and transition width (ΔT) were obtained from the measurement of dc electrical resistivity. The ac magnetic susceptibility was measured to determine the phase transition and to estimate the presence of different phases. The lattice parameter and the percentage of high T_c -phase were determined by X-ray diffraction (XRD) technique. The scanning electron microscopy (SEM) was used to observe the morphological structure of materials.

EXPERIMENTAL

The samples with the nominal composition $\text{Bi}_{2-x}\text{Tl}_x\text{Pb}_{0.4}\text{Sr}_2\text{Ca}_2\text{Cu}_3\text{O}_y$ ($x = 0.00, 0.05, 0.15, 0.25$ and 0.35) were prepared by the conventional solid-state reaction method¹². The stoichiometric amounts of high purity Bi_2O_3 (99.9 %) PbO (99.9+) and SrCO_3 (99.9 %) supplied by Aldrich and CuO (> 99 %), CaCO_3 (99.9 %) Ti_2O_3 (> 99 %) supplied

by Fluka were used as starting materials. The required quantities of the materials were weighed, mixed and ground for 1 h in an electrical grinder (Retch RM100). The mixtures were first calcined in air using a temperature programmed muffle furnace (Vulcan 3-130) initially at 790 °C for 24 h and then 800 °C for 24 h at optimized heating rates¹³ of 14 °C/min. The resulting powders were ground and pelletized at 50 kNm⁻² pressures by a Paul-Weber (PW-30) pellet press. These pellets were sintered in air at 850 °C for 84 h, 845 °C for 12 h, 850 °C for 24 h and then at 860 °C for 24 h in the muffle furnace at the heating rate of 14 °C/min. The samples were allowed the natural furnace cooling. The ac susceptibility of the samples was measured with a laboratory-built ac susceptometer using a lock-in amplifier Stanford (SR-830). The electrical resistivity was measured with a conventional dc four point-probe method¹⁴ employing Janis Research module (VPF-100) combined with a temperature controller (Lakeshore 321). High conductivity silver paint (Agar Scientific) was used for resistivity measurements. Powder X-ray diffraction (XRD) patterns of the samples were obtained with an X-ray diffractometer (JEOL JDX-60PX) which uses CuK_α radiation source of 40 kV and 30 mA with a step of 0.02° over the range of 2-70° and with a scan speed of 8° min⁻¹. The volume percentages of the Bi-2223 and Bi-2212 phases were estimated by measuring the integrated peak intensities of the major XRD peaks¹⁵.

RESULTS AND DISCUSSION

Fig. 1 represents the XRD patterns of Tl-doped samples (Bi_{2-x}Tl_xPb_{0.4}Sr₂Ca₂Cu₃O_y, where x = 0.0, 0.05, 0.15, 0.25 and 0.35). The characteristic reflection peak intensities and their corresponding miller indices (hkl) are listed in Table-1. All the prepared samples consist of mainly a high-T_c (2223) phase and a low-T_c (2212) phase. For an undoped sample, the characteristic peak H (002) for Bi-2223 phase appears at 2θ = 4.62° (d = 19.111 Å). For the doped samples (x = 0.05 and x =

0.15) the intensity of the lower angle peak decreases gradually and for the sample with x = 0.25 this peak splits into two at 2θ = 4.72° (d = 18.627 Å) and 2θ = 5.68° (d = 15.546 Å) representing the high-T_c Bi-(2223) and low-T_c Bi-(2212) phase, respectively. For sample x = 0.35, peak intensity corresponding to the high-T_c phase disappears and only a single peak is observed at 2θ = 5.9° (d = 14.967 Å) that represents the low-T_c phase. As has been observed in our samples, peaks corresponding to the high- and low-T_c phases at lower angle have been reported previously¹⁶. The variation in XRD peak intensity and lattice parameter “c” provides information of inter-atomic distance of Cu-O and Bi-O layers which are intimately involved in the superconductivity¹⁷.

TABLE-1
COMPARISON OF 2θ, d-VALUES, CHARACTERISTIC-
PEAK INTENSITIES, H (hkl) AND L (hkl), f(v) OF
Bi_{2-x}Tl_xPb_{0.4}Sr₂Ca₂Cu₃O_y (0 ≤ x ≤ 0.35) SAMPLES

Tl content x	2θ	d-value	Characteristic peak intensities	Phase (hkl)
0.0	4.6	19.11	270	H(002)
	28.8	3.10	659	H(117)
	33.0	2.71	805	H(200)
0.05	4.8	18.27	250	H(002)
	29.0	3.08	862	H(0012)
	33.2	2.69	911	L(200)
0.15	4.6	18.24	203	H(002)
	28.6	3.12	732	L(018)
	32.9	2.72	718	H(200)
0.25	4.7	18.63	129	H(002)
	5.7	15.55	110	L(002)
	27.5	3.25	576	H(116)
	28.8	3.10	506	H(117)
	33.1	2.71	841	H(200)
0.35	5.9	14.97	153	L(002)
	27.7	3.22	1164	L(115)
	31.2	2.96	766	H(1011)
	33.4	2.68	663	H(0112)

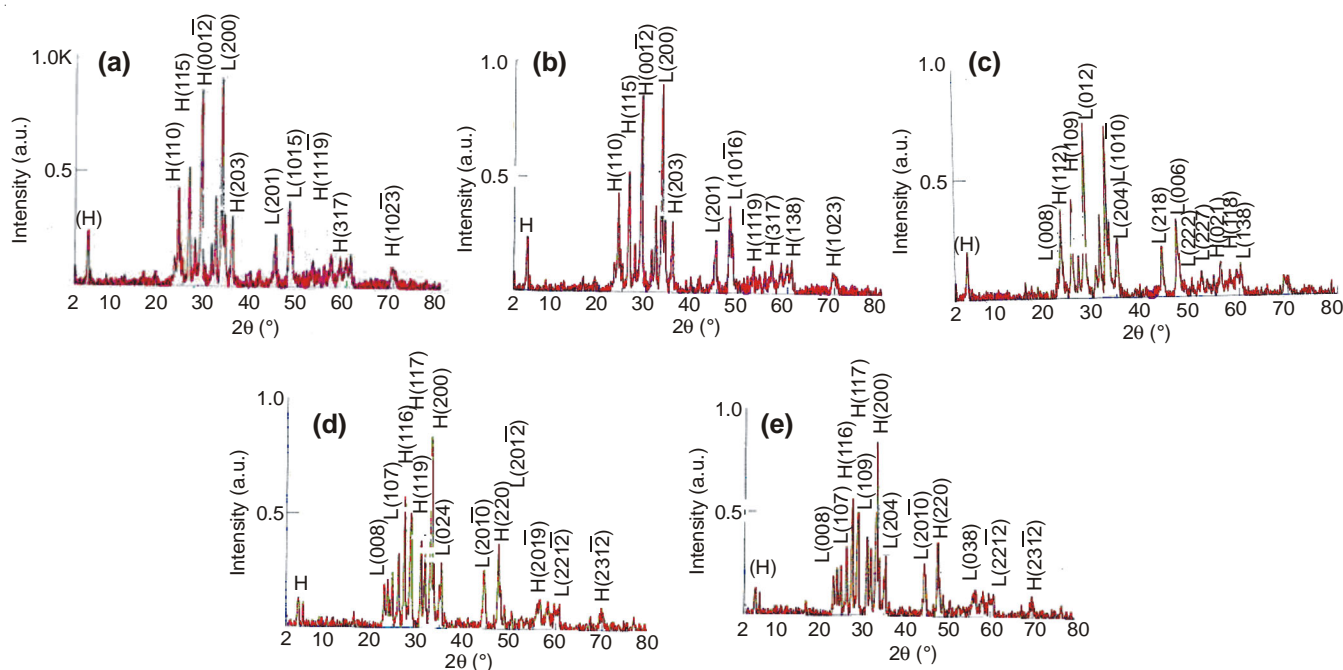


Fig. 1. (a-e) XRD patterns of thallium doped samples Bi_{2-x}Tl_xPb_{0.4}Sr₂Ca₂Cu₃O_y where (x = 0.0, 0.05, 0.15, 0.25 and 0.35)

Fig. 2 shows the temperature dependence of dc electrical resistivity of $\text{Bi}_{2-x}\text{Tl}_x\text{Pb}_{0.4}\text{Sr}_2\text{Ca}_2\text{Cu}_3\text{O}_y$ samples containing different thallium concentrations $x = 0.00, 0.05, 0.15, 0.25$ and 0.35 . The electrical resistivity of these superconducting materials, starts to decrease below room temperature (298 K), they show metallic character in the normal state region and attain a state of zero electrical resistivity at the critical temperature $T_{c(0)}$ (Table-2). The room temperature resistivity of the samples has been determined in the range of (0.012-0.020) ohm-cm. A sample with $x = 0.25$ shows value of $\rho_{(RT)} = 0.0116$ and a sample with $x = 0.05$ exhibit the highest value of $\rho_{(RT)} = 0.020$ (ohm-cm) (Table-2). The addition of thallium in the range of ($0.15 \leq x \leq 0.35$) results in lowering the value of $\rho_{(RT)}$ whereas a minor change in the values of $\rho_{(RT)}$ is observed for the samples containing thallium concentrations of ($0.00 \leq x \leq 0.05$). The slope of the electrical resistivity curves in the normal state region decrease almost in a regular order and show lower values of residual resistivity $\rho_{0(RT)}$ in the former set of samples compared to the latter set of samples. It can be inferred from these results that all the doped samples exhibit comparable [$\rho_{(RT)}$] values and addition of thallium to the bismuth based superconducting materials helps in lowering the room temperature electrical resistivity, improves the metallic behaviour in the normal state regime and also decreases the normal state residual resistivity $\rho_{0(RT)}$. The cause of decrease in room temperature with increase in thallium content can be formation of a uniform phase, better grain connectivity and increase in the charge carrier concentration due to the overlapping of Tl(6s) and Cu-O conduction bands.

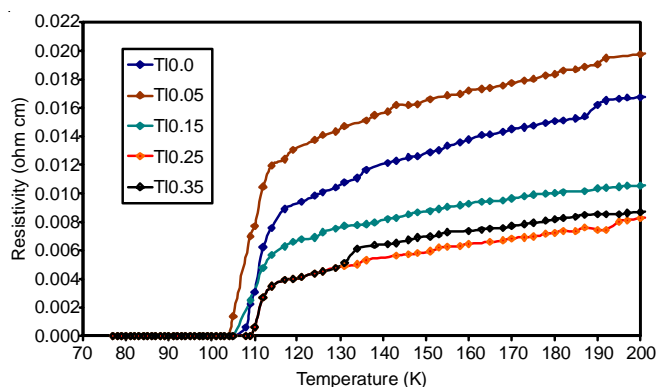


Fig. 2. Electrical resistivity *versus* temperature curves of thallium-doped samples $\text{Bi}_{2-x}\text{Tl}_x\text{Pb}_{0.4}\text{Sr}_2\text{Ca}_2\text{Cu}_3\text{O}_y$ where ($0 \leq x \leq 0.35$)

Thallium content (x)	$\rho_{(RT)}$ (ohm-cm)	$T_{c(\text{onset})}$ (K)	$T_{c(0)}$ (K)	ΔT (K)
0.0	0.014	117	105	12.0
0.05	0.020	114	104	10.0
0.15	0.012	114	105	9.0
0.25	0.012	114	109	5.0
0.35	0.012	112	109	3.0

Except for the undoped sample, the value of $T_{c(\text{onset})}$ of all the doped samples containing different amount of thallium

are in the range of (112-114) (Table-2). These values are determined by the temperature *versus* resistivity graphs given in Fig. 3. The samples with ($x = 0.05, 0.15$ and 0.25) exhibit $T_{c(\text{onset})}$ value of 114 K but a sample with higher Tl content, $x = 0.35$ shows the $T_{c(\text{onset})} = 112$ K. The critical transition temperature, $T_{c(\text{onset})}$ is identified as the transition of the isolated grains to the superconducting state in granular superconductors¹⁸. Its constant value for samples with $x = 0.05, 0.15$ and 0.25 , suggests that the grains are insensitive to the change in dopant concentration in a certain concentration limit. The value of $T_{c(\text{onset})}$ depends not only on the relative volume fraction of the superconducting phases but also on the quality of their inter-granular coupling that can be affected by the presence of impurity phases in the grain boundaries and also by micro cracking in the samples. The minor decrease in the value of $T_{c(\text{onset})}$ for sample with $x = 0.35$ might possibly be due to the reasons described above.

The zero resistivity temperature $T_{c(0)}$ for samples ($0 \leq x \leq 0.35$) lies in the range of (104-109) K (Table-2). Sample with $x = 0.25$ and 0.35 have value of $T_{c(0)} = 109$ K while a sample with $x = 0.05$ exhibits a $T_{c(0)} = 104$ K. It can be noted from the range of $T_{c(0)}$ that overall a high- T_c (2223) phase predominates over the low- T_c (2212) phase in samples containing thallium contents of ($0 \leq x \leq 0.35$). The largest value of $T_{c(0)} = 109$ K for samples with thallium contents of $x = 0.25$ and 0.35 corresponds to the comparable volume percentage of the high- T_c (2223) phase in both samples. The increase in $T_{c(0)}$ with increase in thallium concentration from $x = 0.0$ to 0.25 suggests that thallium enters into the crystal structure that helps overlapping of thallium (6s) with Cu-O conduction bands and thus enhances the overall charge carrier concentration. This ultimately becomes the cause of increase in $T_{c(0)}$ with increase in thallium-content in certain concentration range.

The transition width, ΔT for sample containing Tl-contents of ($0 \leq x \leq 0.35$) has been calculated in the range of (3-12) K (Table-2). For un-doped sample, the value of ΔT is 12 K and it decreases gradually with increase in Tl-content *i.e.* ($0.05 \leq x \leq 0.35$). A regular decrease in the value of (ΔT) suggests that thallium not only increases the $T_{c(0)}$ but also improves the quality of samples and helps in the uniform phase formation and grain connectivity.

Plots of ac susceptibility of various Tl-doped samples measured at different temperatures are shown in Fig. 3(a-e). The magnetic manifestation of zero resistivity is that a material is a superconductor if it exhibits perfect diamagnetic shielding; that is, its susceptibility χ is exactly -1. The sample containing Tl-contents of ($0 \leq x \leq 0.25$) show almost similar temperature *versus* susceptibility curves with some difference of sharpness, broadening and diamagnetic saturation level. The patterns indicate that all the samples consist of high- T_c (2223) phase as a major constituent of the samples along with some impurity phases and low- T_c (2212) phase. A smooth and sharp transition in the susceptibility curve of a sample with $x = 0.25$ determines its better quality in terms of phase formation and grain connectivity. The sample with $x = 0.35$ also exhibits sharp transition before saturation. This trend indicates that the high- T_c (2223) phase dominates over the low- T_c (2212) phase in this sample.

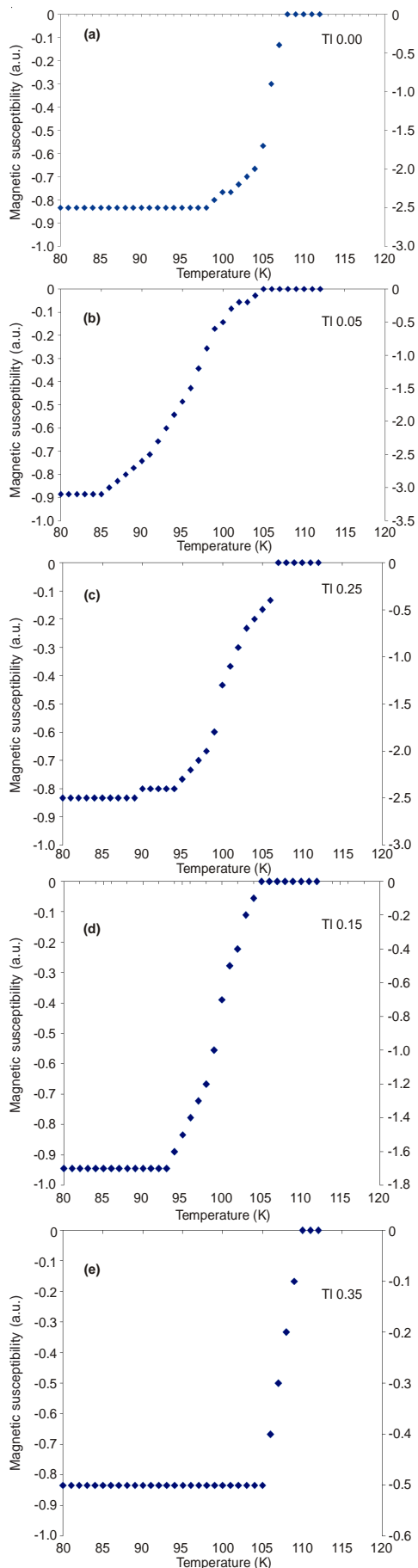


Fig. 3. (a-e) Temperature versus magnetic susceptibility curves of thallium-doped $\text{Bi}_{2-x}\text{Tl}_x\text{Pb}_{0.4}\text{Sr}_2\text{Ca}_2\text{Cu}_3\text{O}_y$ samples where $(0 \leq x \leq 0.35)$

Fig. 4(a-c) represents the scanning electron micrographs of various thallium-doped samples *i.e.* $\text{Bi}_{2-x}\text{Tl}_x\text{Pb}_{0.4}\text{Sr}_2\text{Ca}_2\text{Cu}_3\text{O}_y$ containing different thallium contents $x = 0.05, 0.15$ and 0.35 . It has been observed that all the samples consist of both low and high- T_c phases, however the phase formation improves with increase in thallium-content. The sample with $x = 0.35$ has shown a comparatively better phase formation, most probably consisting of high- T_c (2223) phase.

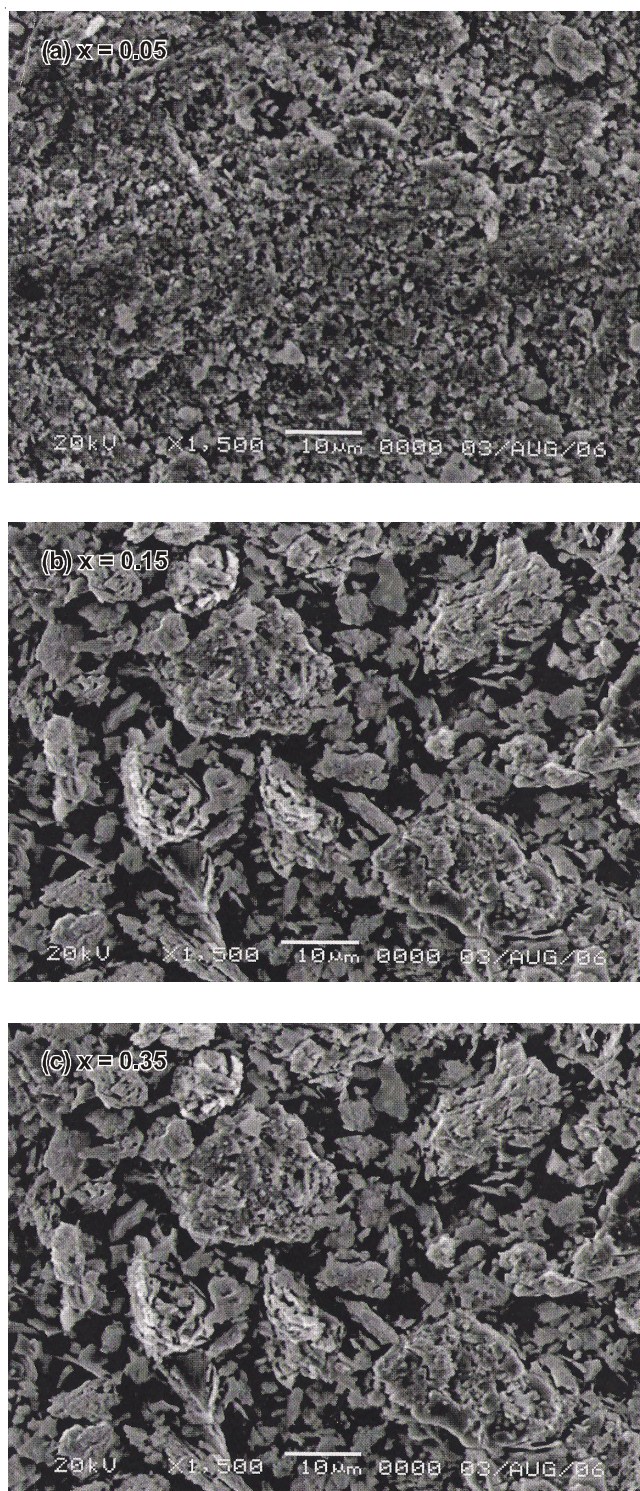


Fig. 4. (a-c) Scanning electron micrographs of thallium-doped $\text{Bi}_{2-x}\text{Tl}_x\text{Pb}_{0.4}\text{Sr}_2\text{Ca}_2\text{Cu}_3\text{O}_y$ samples where $(x = 0.05, 0.15$ and $0.35)$

REFERENCES

1. A.K. Sarkar, I. Maartense, B. Kumar and T.L. Peterson, *Supercond. Sci. Technol.*, **3**, 199 (1990).
2. A.K. Sarkar and I. Maartense, *Solid State Commun.*, **77**, 121 (1991).
3. V. Mihalache, G. Aldica and P. Badica, *Physica C*, **392-396**, 185 (2003).
4. A. Jeremie, K. Alami-Yadri, J.-C. Grivel and R. Flükiger, *Supercond. Sci. Technol.*, **6**, 730 (1993).
5. G.N. Rao and D.S. Babu, *Mater. Chem. Phys.*, **31**, 267 (1992).
6. H.S. Kim, G.J. Lee, J.Y. Lee, D.H. Lee and K.H. Kim, *Mater. Chem. Phys.*, **49**, 12 (1997).
7. G. Liang, Q. Yao, S. Zhou and D. Katz, *Physica C*, **424**, 107 (2005).
8. H.M. Seyoum, J.M. Habib, L.H. Bennett, W. Wong-Ng, A.J. Shapiro and L.J. Swartzendruber, *Supercond. Sci. Technol.*, **3**, 616 (1990).
9. K. Watanabe and N.K. Kojima, *Supercond. Sci. Technol.*, **11**, 392 (1998).
10. J.-C. Grivel, A. Jeremie and R. Flükiger, *Supercond. Sci. Technol.*, **8**, 41 (1995).
11. D.R. Mishra, P.L. Upadhyay and R.J. Sharma, *Physica C*, **304**, 293 (1998).
12. H. Maeda, Y. Tanaka, M. Fukutomi and T. Asano, *Jpn. J. Appl. Phys.*, **27**, L209 (1988).
13. M.J. Iqbal and R. Mehmood, *J. Am. Ceram. Soc.*, **91**, 1019 (2008).
14. C. Terzioğlu, M. Yilmazlar, O. Oztürk and E. Yanmaz, *Physica C*, **423**, 119 (2005).
15. I. Karaca, S. Celebi, A. Varilci and A.I. Malik, *Supercond. Sci. Technol.*, **16**, 100 (2003).
16. D.R. Mishra, P.L. Upadhyay and R.J. Sharma, *Physica C*, **304**, 293 (1998).
17. Y. Li, G. Cao, R. Ma and Z. Zhao, *Solid State Commun.*, **79**, 491 (1991).
18. E. Govea-Alcaide, R.F. Jardim and P. Muné, *Physica C*, **423**, 152 (2005).